Available online at www.sciencedirect.com

ScienceDirect

Ceramics International 38 (2012) 817–819

CERAMICS INTERNATIONAL

www.elsevier.com/locate/ceramint

Short Communication

Investigation of planar defects in pulsed electric current sintered $B_{13}C_2$ boron carbide ceramic

Song Zhang [a,*], Wenzhong Lu [a], Chuanbin Wang [b], Qiang Shen [b], Lianmeng Zhang [b]

[a] *Department of Electronic Science and Technology, Huazhong University of Science and Technology, 1037 Luoyu Road, Wuhan 430074, People's Republic of China*

[b] *State Key Laboratory of Advanced Technology for Materials Synthesis and Processing, Wuhan University of Technology, Wuhan 430070, People's Republic of China*

Received 13 June 2011; received in revised form 21 July 2011; accepted 21 July 2011

Abstract

$B_{13}C_2$ boron carbide ceramic was prepared by pulsed electric current sintering from raw element boron and graphite powders. The planar defects in (1 0 4) planes were investigated by transmission electron microscopy and X-ray photoelectron spectroscopy. The results showed the B_{12} C–B–C configuration of $B_{13}C_2$ ceramic agreed well with C_{1s} spectra measurement. The weakly linked C–B–C chains made the atomic disorder in (1 0 4) planes which led to defects in these planes.

Keywords: $B_{13}C_2$ boron carbide; Planar defects; Transmission electron microscopy; X-ray photoelectron spectroscopy

Boron carbide is an interesting material in many of potential applications, such as an abrasive and superhard material [1], a thermoelectric device material [2] and control rods for nuclear power generation [3]. Boron carbide is nominally assigned the formula B_4C, although it has a wide range from B_4C to $B_{10.5}C$ and corresponding to a composition range of about 20–9 at.%C, respectively [4]. This large range of composition leads to the presence of atomic disordered and planar defects [5–7]. The nature of disordering mechanisms have been extensively investigated and hotly debated [7–10] and experimental determination of the atomic structure for $B_{13}C_2$ is still lacking. It is valuable to investigate the formation mechanism of planar defects because these defects play an important role in electrical and thermal application of $B_{13}C_2$ [11].

Although the general structural features of boron carbide are defined like that boron carbide crystallizes in a rhombohedral structure with space group *R*-3*m* [12], consisting of a 12-atom icosahedrons and 3-atom chain distributed over four positions: equatorial sites along the center of the icosahedrons, polar sites that form the two triangular caps of the icosahedrons, the two ends of the 3-atom chain, and the center of the chain. However, the details of fine-structure of boron carbide are still not understood clearly, especially $B_{13}C_2$. In the early years, Emin [4] suggested the structure of B–C materials as composition became more boron rich, the $B_{11}C$ icosahedra in B_4C initially retained its carbon while one of the carbons on the C–B–C chains was gradually replaced by boron. Near the composition $B_{13}C_2$, the structure consists of $B_{11}C$ icosahedra and C–B–B chains, with further carbon reduction, the $B_{11}C$ icosahedra were replaced by B_{12} icosahedra while the chains remained C–B–B. Interpretations of Raman spectra [13], infrared spectra [14], and neutron powder diffraction [15] are consistent with Emin model. Whereas, in recent years, there were disagreements about structure of boron carbide at 13.33 at.%C ($B_{13}C_2$), Saal et al. [12] and Fanchini et al. [16] investigated fine structure of $B_{13}C_2$ by formation enthalpy and Gibbs free-energy calculations, respectively. And their results supported that there was a three-atom C–B–C chain in $B_{13}C_2$ with B_{12} icosahedra.

In this study, $B_{13}C_2$ boron carbide ceramic was prepared by pulsed electric current sintering. The planar defects in (1 0 4) planes of $B_{13}C_2$ boron carbide ceramic were investigated by transmission electron microscopy and X-ray photoelectron spectroscopy.

The $B_{13}C_2$ boron carbide ceramic was prepared via pulsed electric current sintering from raw element boron and graphite powders. The more sintering details can be found in our former

---

* Corresponding author.
E-mail address: superkobe0104@hotmail.com (S. Zhang).

0272-8842/$36.00 © 2011 Elsevier Ltd and Techna Group S.r.l. All rights reserved.
doi:10.1016/j.ceramint.2011.07.040

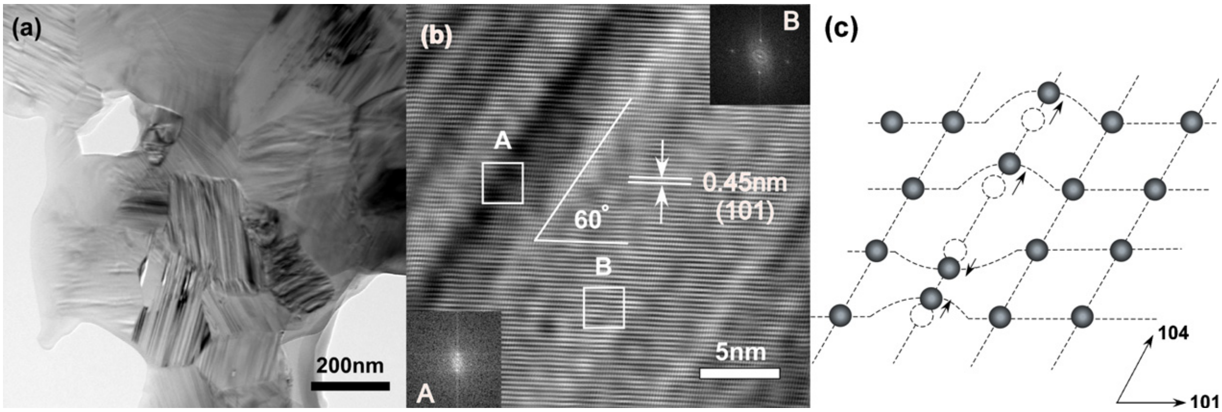

Fig. 1. TEM images of the $B_{13}C_2$ boron carbide ceramic (a) bright-field image (b) high resolution image and FFT patterns and (c) schematics for displacements in (1 0 4) planes.

report [17]. Sintered $B_{13}C_2$ sample was cut in half, one half was prepared for TEM (JEOL, JEM-2010, operated at 200 kV) observation via standard dimpling and ion-milling, the other one was grinded to powders for XPS (ESCA Lab. MK II spectrometer) measurement. The XPS signal was analyzed using a peak synthesis program in which a nonlinear background was assumed and the fitting peaks of the experimental curve were defined. The spectrums were analyzed with their deconvolution and Shirley background fitting. The fitting function was a combination of Gaussian (77%) and Lorentzian (23%) distributions.

A high density of striations can be observed in the $B_{13}C_2$ grains as shown in Fig. 1(a). The presence of such features in sintered B_4C has been observed in previous reports [6,10] and those striations have been identified as planar defects (e.g. twins, planar stacks and amorphous bands) by TEM studies. From the high resolution image, Fig. 1(b), it can be concluded that the striations are tilted by approximately 60° with (1 0 1) planes. After calculation, result shows that the striations are parallel to (1 0 4) planes. Furthermore, selected area electronic diffraction (SAED) method has been used on the two boxed areas (box A and B) for comparison. A diffuse halo, a typical feature of amorphous material, is visible in the pattern of box A. In contrast, pattern of box B shows spot reflections indicative of crystal structure. Additionally, some displacements occurs randomly in (1 0 4) planes as shown as Fig. 1(c) which elucidate planar defects to lie (1 0 4) planes.

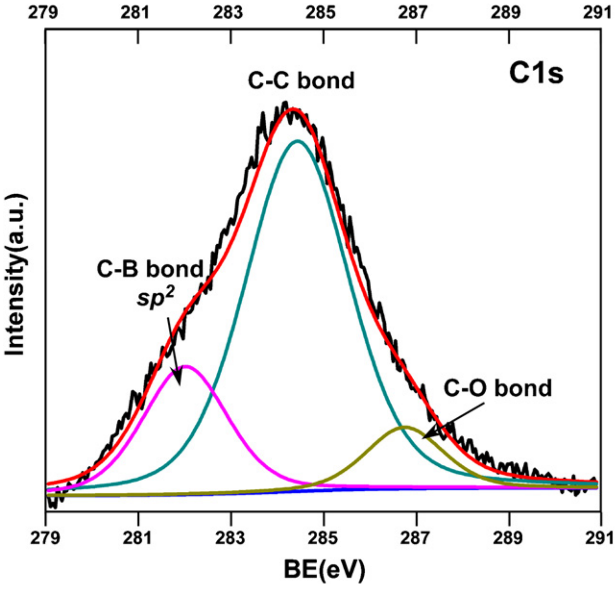

Fig. 2. XPS spectroscopy for C_{1s}.

In order to further confirm the lattice configuration and formation mechanism of planar defects, we analyzed the location of the C atom in $B_{13}C_2$ lattice by XPS. As previous reported, in the case of the C_{1s} spectra in boron carbide, oxides occur at the highest binding energies (C–O at ~286 eV; C=O at ~288 eV) [18], C–C bonds at ~284.6 eV [19], Jiménez et al. [20] identified two chemical environments of carbon atoms which bonded with boron atoms in polycrystalline boron carbide in the C_{1s} spectra, C–B bonds from C atoms in C–B–C chains at ~281.8 eV (sp^2 hybridization) and in the icosahedra at ~283.7 eV (sp^3 hybridization). Fig. 2 presents the C_{1s} spectra measurement obtained after sputter-cleaning of the surface of the sample. Obviously, the most intense peak is at 284.6 eV in addition to a low BE (binding energy) and a high BE shoulders. After deconvolution and Shirley background fitting, the C_{1s} spectrum is unsymmetrical and well fit by three chemical environments centered at ~281.8 eV, 284.6 eV and 286.9 eV which are attributed to C–B bonds (sp^2 hybridization), C–C bonds and C–O bonds as labeled in Fig. 2, respectively. Hence, the two carbon atoms in $B_{13}C_2$ are all in the central chain, not in icosahedrons because of absence of the chemical environment of sp^3 hybridization (at ~283.7 eV). The results imply that the $B_{13}C_2$ has a structure of B_{12} C–B–C in this study which supports the calculations of Saal et al. and Fanchini et al. Two higher BE peaks are assigned to C–C and C–O bonding which caused by the hydrocarbons from pump oil adsorbed at sample surface or/and remained free carbide in sample [17] and the adherence of O atoms on the sample surface, respectively.

Boron carbide structure consists of almost regular icosahedra of 12 atoms cross-linked by 3-atom chains as shown in Fig. 3. There are only chain central atoms lying in (1 0 4) planes after cleave $B_{13}C_2$ lattice parallel to (1 0 4) planes which planar defects occur in this study. On the other hand, Kwei and Morosin [8] said that the bonding to the central atom is very weak in the three-atom C–B–C chains in the boron carbide. Tucker and Senio

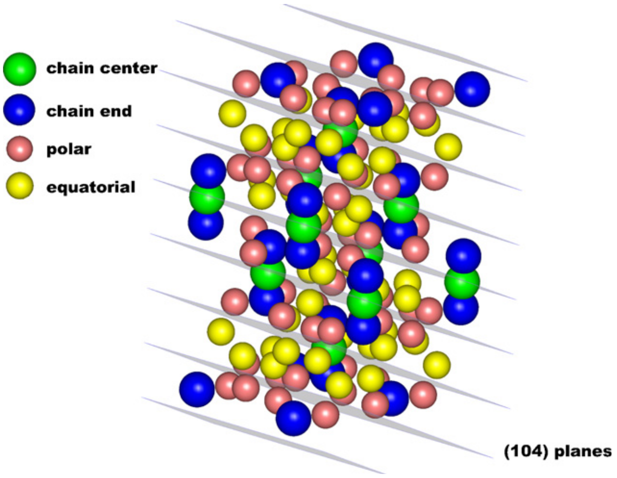

Fig. 3. (1 0 4) planes of $B_{13}C_2$ cell.

[21] described the C–B–C chains as ''soft and weak'' with a neutron irradiation study. They found that a large number of defects were formed at the chain central sites which must be weakly bound compared with the more strongly bonded icosahedral atoms. From the results outlined above, the presence of (1 0 4) planar defects which shown as a high density of striations due to a combination of three factors: (1) (1 0 4) planes are filled with boron atoms at chain central sites only. (2) Atomic disorder in (1 0 4) planes may be caused by chain central boron with weak bond in C–B–C chain. (3) High temperature and mechanical stress provided by PECS equipment lead to the displacement of the weakly bonded atoms during the sintering.

Additionally, it is interesting to notice that whether C–C–B chains consisted in $B_{13}C_2$ sample or not. Generally, C–C bonding in C_{1s} spectra is defined as the hydrocarbons from pump oil adsorbed at sample surface or other kind of adventitious carbon. However, C–C–B chains which few researchers focuses on could also provide a C–C environment. If C–C–B chains existed in $B_{13}C_2$ sample, the 3-atom chains would be failed even more easily [16]. Unfortunately, it is very difficult for XPS to distinguish the slight difference between C–C bonds in adventitious carbon and in C–C–B chains.

In summary, TEM and XPS are applied to investigate the mechanism of the defects in (1 0 4) planes in pulsed electric current sintered $B_{13}C_2$ sample. The structural arrangement for $B_{13}C_2$ boron carbide ceramic is different from Emin's model in this work. For this ceramic, two carbon atoms are all in the 3-atom chain with lattice structure appears to be B_{12} C–B–C. High temperature and mechanical stress provide by PECS equipment in sintering process lead to the displacement of the chain central site atom because of loose bonds. Further, the atomic displacement in (1 0 4) planes causes a high density of defects in $B_{13}C_2$ grains.

Acknowledgement

This research was sponsored by National Nature Science Foundation of China, No. 51102101.

References

[1] L.G. Jacobsohn, R.D. Averitt, C.J. Wetteland, R.K. Schulze, M. Nastasi, L.L. Daemen, Z. Jenei, P. Asoka-kumar, Role of intericosahedral chains on the hardness of sputtered boron carbide films, Appl. Phys. Lett. 84 (2004) 4173.

[2] S. Sasaki, M. Takeda, K. Yokoyama, T. Miura, T. Suzuki, H. Suematsu, W. Jiang, K. Yatsui, Thermoelectric properties of boron-carbide thin film and thin film based thermoelectric device fabricated by intense-pulsed ion beam evaporation, Sci. Technol. Adv. Mater. 6 (2005) 181.

[3] M.W. Chen, J.W. McCauley, K.J. Hemker, Shock-induced localized amorphization in boron carbide, Science 299 (2003) 1563.

[4] D. Emin, Structure and single-phase regime of boron carbides, Phys. Rev. B 38 (1988) 6041.

[5] R. Lazzari, N. Vast, J.M. Besson, S. Baroni, A. Dal Corso, Atomic structure and vibrational properties of icosahedral B_4C boron carbide, Phys. Rev. Lett. 83 (1999) 3230.

[6] E.M. Heian, S.K. Khalsa, J.W. Lee, Z.A. Munir, Synthesis of dense, high-defect-concentration B_4C through mechanical activation and field-assisted combustion, J. Am. Ceram. Soc. 87 (2004) 779.

[7] A.-T. Umberto, M. Ohyanagi, Z.A. Munir, Modeling studies of the effect of twins on the X-ray diffraction patterns of boron carbide, Chem. Mater. 16 (2004) 4347.

[8] G.H. Kwei, B. Morosin, Structures of the boron-rich boron carbide from neutron powder diffraction: implications for the nature of the inter-icosahedral chains, J. Phys. Chem. 100 (1996) 8031.

[9] U. Kuhlmann, H. Werheit, K.A. Schwetz, Distribution of carbon atoms on the boron carbide structure elements, J. Alloys Compd. 189 (1992) 249.

[10] T.L. Aselage, D. Emin, L. Kleinman, Conductivities and Seebeck coefficients of boron carbide: softening bipolaron hopping, Phys. Rev. B 64 (2001) 054302.

[11] R. Schmechel, H. Werheit, Correlation between structural defects and electronic properties of icosahedral boron-rich solids, J. Phys.: Condens. Matter 11 (1999) 6803.

[12] J.E. Saal, S. Shang, Z.K. Liu, The structural evolution of boron carbide via ab initio calculations, Appl. Phys. Lett. 91 (2007) 231915.

[13] D. Tallant, T.L. Aselage, A. Campbell, D. Emin, Boron carbide structure by Raman spectroscopy, Phys. Rev. B 40 (1989) 5649.

[14] E. Pascual, E. Martinez, J. Esteve, A. Lousa, Boron carbide thin films deposited by tuned-substrate RF magnetron sputtering, Diam. Relat. Mater. 8 (1999) 402.

[15] B. Morosin, G.H. Kwei, A.C. Lawson, T.L. Aselage, D. Emin, Neutron powder diffraction refinement of boron carbides nature of intericosahedral chains, J. Alloys Compd. 226 (1995) 121.

[16] G. Fanchini, J.W. McCauley, M. Chhowalla, Behavior of disordered boron carbide under stress, Phys. Rev. Lett. 97 (2006) 035502.

[17] S. Zhang, W. Lu, C. Wang, Q. Shen, L. Zhang, Synthesis and characterization of $B_{13}C_2$ boron carbide ceramic by pulsed electric current sintering, Ceram. Int. (2010), doi:10.1016/j.ceramint.2011.05.036.

[18] O. Postel, J. Heberlein, Deposition of boron carbide thin film by supersonic plasma jet CVD with secondary discharge, Surf. Coat. Technol. 108–109 (1998) 247.

[19] L.G. Jacobsohn, R.K. Schulze, M.E.H. Maia da Coasta, M. Nastasi, X-ray photoelectron spectroscopy investigation of boron carbide films deposited by sputtering, Surf. Sci. 572 (2004) 418.

[20] I. Jiménez, D.G.J. Sutherland, T. van Buuren, J.A. Carlisle, L.J. Terminello, Photomemission and X-ray-absorption study of boron carbide and its surface thermal stability, Phys. Rev. B 57 (1998) 13167.

[21] C.W. Tucker, P. Senio, X-ray scattering by neutron-irradiated single crystals of boron carbide. I, Acta Crystallogr. 8 (1955) 371.